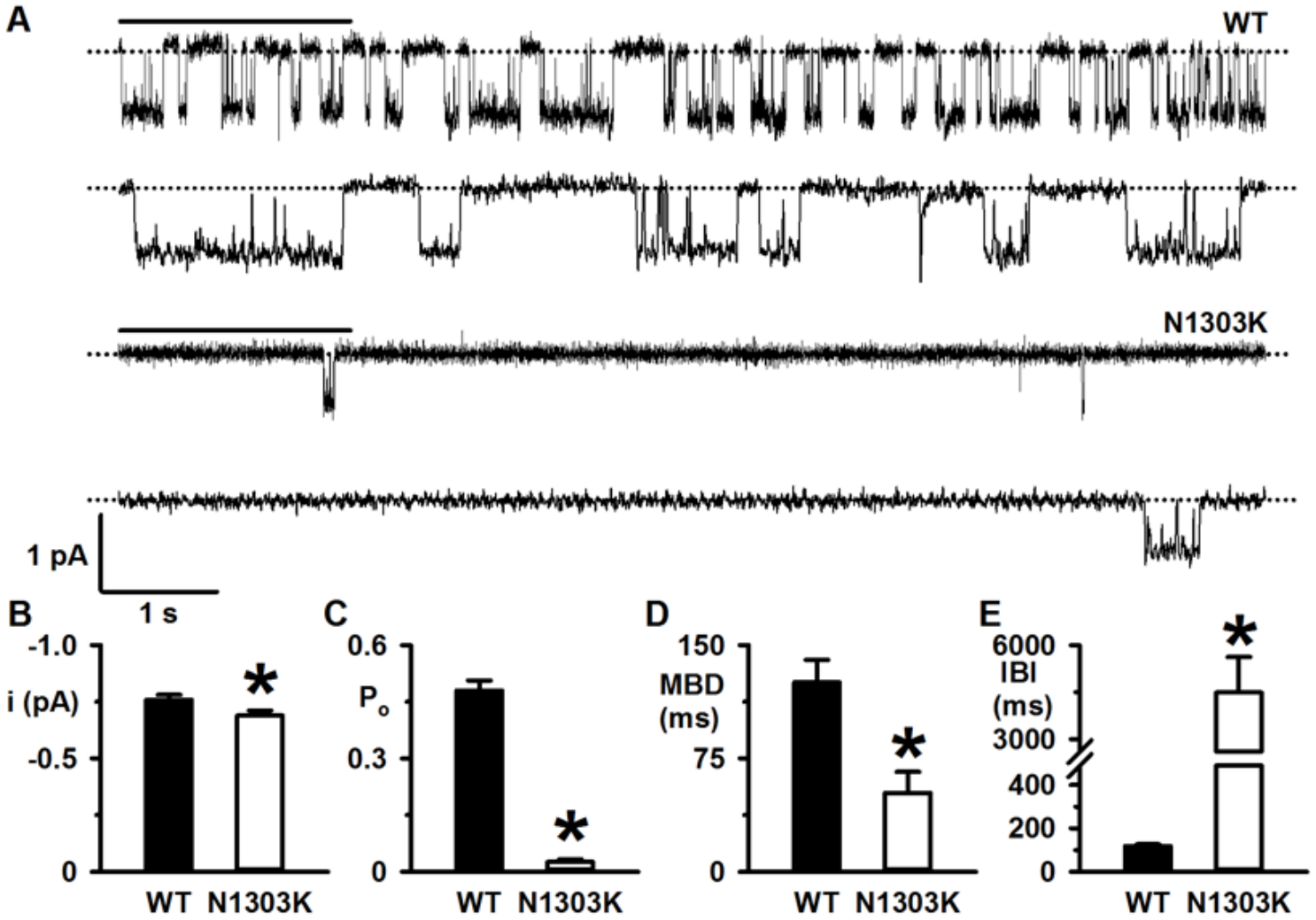

Supplemental Figure 1. Effects of ivacaftor on the N1303K-CFTR channel gating defect
(**A**) Representative single-channel recordings of WT- and N1303K-CFTR in excised inside-out membrane patches from transiently transfected CHO cells show the effects of ivacaftor (VX-770; 1 μM) on the N1303K variant. ATP (1 mM) and PKA (75 nM) were continuously present in the intracellular solution. Dotted lines indicate the closed channel state and downward deflections correspond to channel openings. (**B – E**) Single-channel current amplitude (i), open probability (P_o), mean burst duration (MBD) and interburst interval (IBI) of WT- and N1303K-CFTR. Data are means ± SEM (WT, i and P_o, n = 8, MBD and IBI, n = 6; N1303K, i and P_o, n = 6, MBD and IBI, n = 5); *, $p < 0.05$ vs. WT-CFTR; †, $p < 0.05$ vs. N1303K-CFTR control.

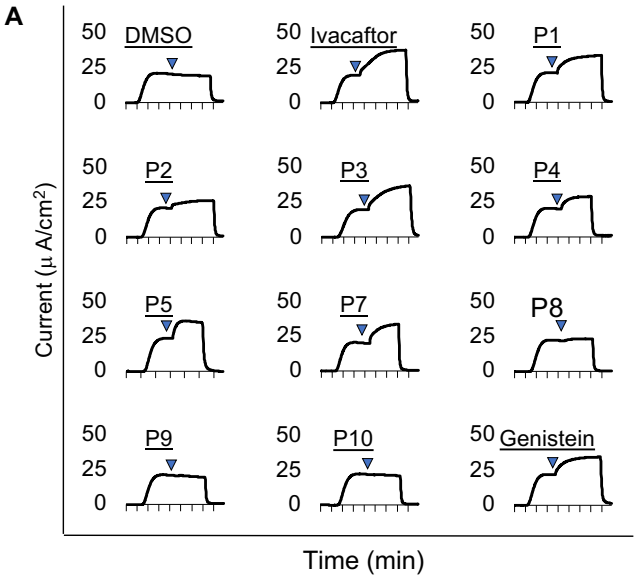

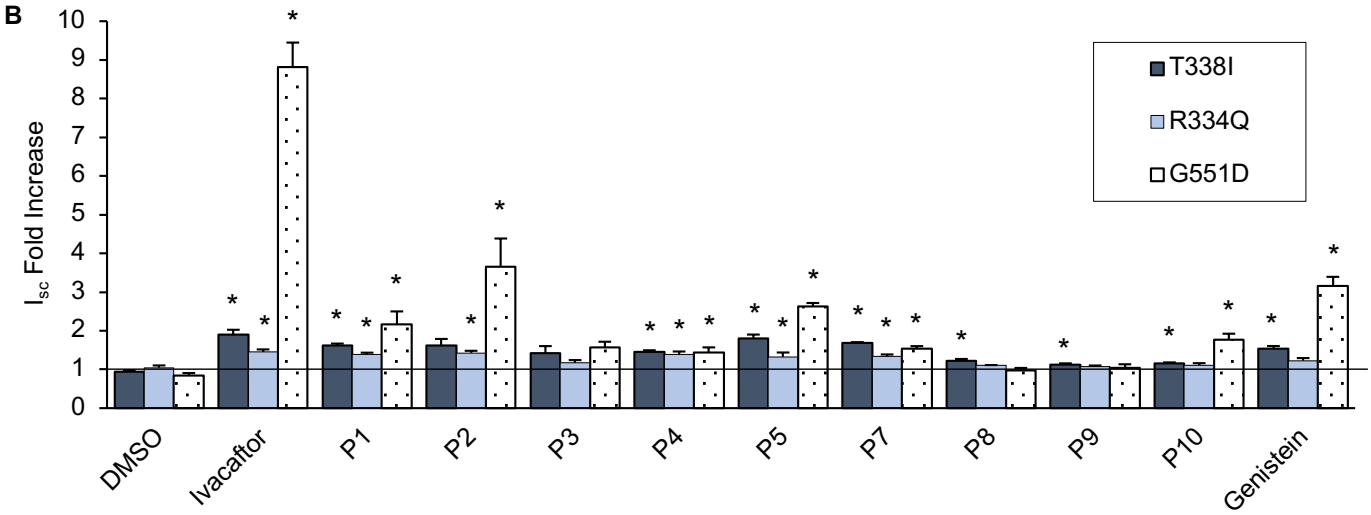

Supplemental Figure 2. Testing alternative potentiator compounds
(**A**) Representative I_{sc} tracings for T338I treated with 10 different potentiators compounds compared to ivacaftor and DMSO presented as area corrected current ($\mu A/cm^2$), over time, measured in minutes represented by tick marks in 1 min intervals. (**B**) Summary data for T338I and R334Q treated with potentiator panel compared to G551D. Line indicates no change compared to untreated cells. Error bars represent ± SEM, * = $p<0.05$

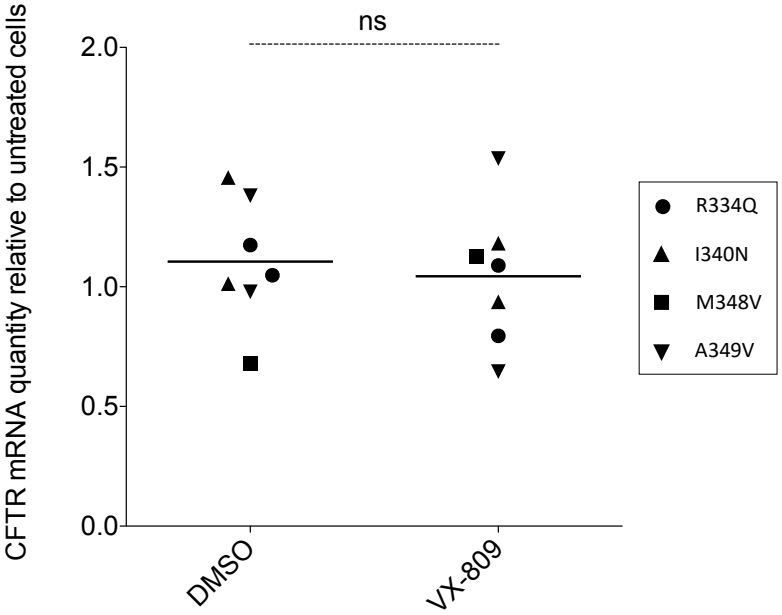

Supplementary Fig 3. Effects of 24 h treatment with 6 μM lumacaftor or equal volume DMSO on CFTR mRNA expression

CFTR mRNA expression from lumacaftor or an equal volume of DMSO treated cells were compared to untreated cells prepared in parallel for 4 variants performed twice each. Significance tested by 2 tailed unpaired t-test.

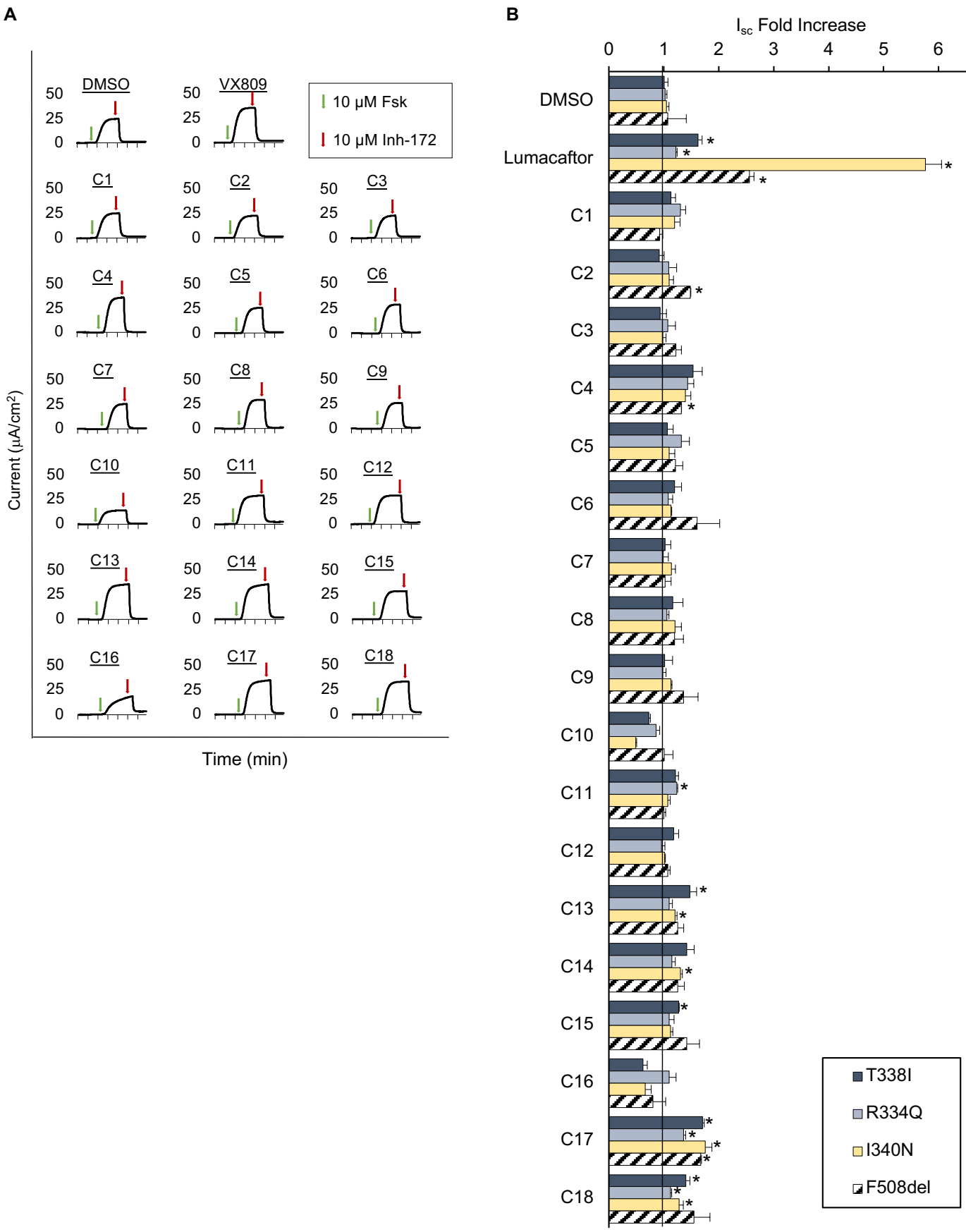

Supplemental Figure 4. Testing alternative corrector compounds
(**A**) Representative I_{sc} tracings for forskolin (Fsk) stimulated currents of T338I treated with 18 different corrector compounds compared to lumacaftor and DMSO presented as area corrected current (μA/cm^2), over time, measured in minutes represented by tick marks in 1 min intervals. (**B**) Summary of response of T338I, R334Q, I340N, and F508del to corrector panel and DMSO compared to untreated cells. Line indicates no change compared to untreated cells. Error bars represent ± SEM, * = $p<0.05$

Confirmation of plasmid integration

Integration of *CFTR* variant plasmids was evaluated by extraction of genomic DNA from hygromycin resistant cell lines and PCR amplification of the entire *CFTR* cDNA as well as of an empty flp recombinase target integration site. Cell lines containing the entire *CFTR* cDNA, with an interrupted flp recombinase target site, were expanded for further testing.

Measuring CFTR expression

Cells ($3x10^5$) for RNA extraction were plated in flat bottom 6 well plates and cultured for 6 days. Total RNA was extracted using the SpinSmart RNA Mini Purification kit (Denville) according to manufacturer's protocol and 500 ng was used for generation of a first strand cDNA library using the iScript cDNA Synthesis Kit (BioRad) according to manufacturer's protocol. Quantitative Real Time PCR (qRT-PCR) was performed with the SsoAdvanced Universal SYBR Green Supermix reagent (BioRad) using 2 primer sets within the *CFTR* cDNA sequence as well as internal primers for the housekeeping gene *HPRT1*; *B2M*, *GUSB*, *GAPDH*, and *TBP* were also evaluated as housekeeping genes, but *HPRT1* was determined to have the most stable expression under our test conditions. Cells were discarded if they failed to demonstrate measurable CFTR expression, lower limit of detection was approximately 7 cycles higher than *HPRT1*.

I_{sc} buffer composition for CFBE cells

The apical buffer contained 145 mM NaGluconate, 1.2 mM $MgCl_2$, 1.2 mM $CaCl_2$, 10 mM dextrose, 10 mM HEPES, and the basolateral buffer was composed of 145 mM

NaCl, 1.2 mM $MgCl_2$, 1.2 mM $CaCl_2$, 10 mM dextrose, 10 mM HEPES. Buffers were pH adjusted to 7.3 using NaOH and warmed to 37 °C prior to use. Air was gently bubbled through chambers to promote circulation.

I_{sc} buffer composition for FRT cells

Low chloride Ringer`s solution (1.2 mM NaCl, 140 mM Na-gluconate, 25 mM $NaHCO_3$, 3.33 mM KH_2PO_4, 0.83 mM K_2HPO_4, 1.2mM $CaCl_2$, 1.2 mM $MgCl_2$, 10 mM glucose) bathing the apical surface and physiological Ringer's solution (120 mM NaCl, 25 mM $NaHCO_3$, 3.33 mM KH_2PO_4, 0.83 mM K_2HPO_4, 1.2 mM $CaCl_2$, 1.2 mM $MgCl_2$, 10 mM glucose) bathing the basolateral surface.

Western Blots of Transiently Transfected Cells

Biochemical effects of small molecules on the expression of CFTR protein were evaluated by Western blot analysis (1, 2). For Western blots of transiently transfected CFTR expression plasmids, we used 40 μg of total lysate collected from HEK293 cells 48 hours post transfection. CFTR was detected using the mouse anti-CFTR monoclonal antibody (596), which recognizes NBD2 of human CFTR (3). Blots were probed with 596 at a concentration of 1:5,000 and secondary anti-mouse antibody at a concentration of 1:100,000.

Calculation of %WT function of CFBE cell lines

Briefly, the slope derived from the correlation between mRNA level (x) and short circuit current (I_{sc}) in $\mu A/cm^2$ (y) for 24 cell lines expressing WT-CFTR is expressed as

y=242.61(x) (4). This is the slope for 100% function. The CFTR mRNA level of each variant ($mRNA_{var}$) is determined by normalizing against the mRNA level of the housekeeping gene *HPRT1* which are each expressed at similar levels in all cell lines. Using the I_{sc} generated by each variant ($I_{sc\text{-}var}$), the % CFTR function of a variant relative to WT-CFTR (F_{var}) is calculated as follows:

$$F_{var}=100\% \text{ X } (I_{sc\text{-}var}/242.61\ (mRNA_{var})) \qquad \text{Eq. 1}$$

Calculation of %WT function of FRT cell lines

Briefly, cell lines were selected that had a very similar level of mRNA expression as cells lines expressing WT-CFTR (0.5 – 1.5 fold) so that %WT function of the variant was derived after dividing the current generated in the cell line expressing the variant by the current generated by the cell line expressing WT CFTR.

CFTR single-channel studies

CFTR Cl^- channels were recorded in excised inside-out membrane patches from CHO cells co-expressing CFTR and GFP voltage-clamped at –50 mV as described previously (5). Prior to experiments, the plasma membrane expression of N1303K-CFTR was rescued by incubating transfected CHO cells at 27 °C for 3 – 7 days. The pipette (extracellular) solution contained (mM): 140 N-methyl-D-glucamine (NMDG), 140 aspartic acid, 5 $CaCl_2$, 2 $MgSO_4$ and 10 N-tris[hydroxymethyl]methyl-2-aminoethanesulfonic acid (TES) adjusted to pH 7.3 with Tris ([Cl^-], 10 mM). The bath (intracellular) solution contained (mM): 140 NMDG, 3 $MgCl_2$, 1 CsEGTA and 10 TES,

adjusted to pH 7.3 with HCl ($[Cl^-]$, 147 mM; free $[Ca^{2+}]$, < 10^{-8} M) and was maintained at 37 °C.

CFTR Cl^- channels were activated promptly following membrane patch excision using the catalytic subunit of protein kinase A (PKA [purified from bovine heart] 75 nM; Calbiochem) and ATP (1 mM; Sigma-Aldrich). To minimize channel rundown, PKA and ATP were added to all intracellular solutions. Because of the difficulty removing ivacaftor from the recording chamber (6) specific interventions with the drug were compared with pre-intervention controls. In this study, membrane patches contained ≤ 5 active channels determined using the maximum number of simultaneous channel openings observing the precautions described previously (7) to minimize errors counting channels.

After recording, filtering and digitizing data (5), single-channel current amplitude (i), P_o, mean burst duration (MBD) and interburst interval (IBI) were determined as described previously (5, 7). For wild-type CFTR, we used only membrane patches with a single active CFTR Cl^- channel for burst analyses, whereas for N1303K-CFTR, we used only bursts of single-channel openings with no superimposed openings from membrane patches with ≤ 4 active channels (8).

Supplemental References

1. Gottschalk LB, Vecchio-Pagan B, Sharma N, Han ST, Franca A, Wohler ES, et al. Creation and characterization of an airway epithelial cell line for stable expression of CFTR variants. *J Cyst Fibros.* 2016;15(3):285-94.
2. Sabusap CM, Wang W, McNicholas CM, Chung WJ, Fu L, Wen H, et al. Analysis of cystic fibrosis-associated P67L CFTR illustrates barriers to personalized therapeutics for orphan diseases. *JCI Insight.* 2016;1(14).
3. Cui L, Aleksandrov L, Chang XB, Hou YX, He L, Hegedus T, et al. Domain interdependence in the biosynthetic assembly of CFTR. *J Mol Biol.* 2007;365(4):981-94.
4. Raraigh KS, Han ST, Davis E, Evans TA, Pellicore MJ, McCague AF, et al. Functional Assays Are Essential for Interpretation of Missense Variants Associated with Variable Expressivity. *Am J Hum Genet.* 2018.
5. Cai Z, Palmai-Pallag T, Khuituan P, Mutolo MJ, Boinot C, Liu B, et al. Impact of the F508del mutation on ovine CFTR, a Cl- channel with enhanced conductance and ATP-dependent gating. *J Physiol.* 2015;593(11):2427-46.
6. Wang Y, Liu J, Loizidou A, Bugeja LA, Warner R, Hawley BR, et al. CFTR potentiators partially restore channel function to A561E-CFTR, a cystic fibrosis mutant with a similar mechanism of dysfunction as F508del-CFTR. *Br J Pharmacol.* 2014;171(19):4490-503.
7. Cai Z, Taddei A, and Sheppard DN. Differential sensitivity of the cystic fibrosis (CF)-associated mutants G551D and G1349D to potentiators of the cystic fibrosis transmembrane conductance regulator (CFTR) Cl- channel. *J Biol Chem.* 2006;281(4):1970-7.
8. Xu Z, Pissarra LS, Farinha CM, Liu J, Cai Z, Thibodeau PH, et al. Revertant mutants modify, but do not rescue, the gating defect of the cystic fibrosis mutant G551D-CFTR. *J Physiol.* 2014;592(9):1931-47.